Comparative Analysis of Two Methods for Instrumental Intensity Estimations Using the Database Accumulated During Recent Large Earthquakes in Japan

Vladimir Sokolov[a] and Takashi Furumura[b]

A database containing records from nine large earthquakes in Japan, obtained by K-NET and KIK-net strong motion stations, was used for the analysis of two techniques for the estimation of instrumental seismic intensity from accelerograms. The first technique is the standard method for JMA intensity evaluation from filtered three-component accelerograms. The second technique is the so-called FAS-intensity, which was developed for MM and MSK scales and which is based on the correlation between levels of the Fourier Amplitude spectrum (FAS) and observed intensity. The relation between these two types of instrumental intensities (JMA_I and spectral MM_I) may be described by linear function for intensities larger than JMA_I 3.5–4 and MM_I 5.0–5.5, but large discrepancy arises at small intensities. The variation is most probably caused by differences in the spectral content of the ground motions, since the JMA_I calculation is sensitive to the spectral amplitude within a narrow frequency band around 0.5 Hz. [DOI: 10.1193/1.2923918]

INTRODUCTION

Seismic intensity scales are widely used for simple and fast estimation of damage levels after an earthquake, as well as for seismic loss assessment. At present several techniques have been proposed for the evaluation of intensity using recorded strong ground motion parameters. These techniques for so-called "instrumental intensity" estimation utilize peak amplitudes of horizontal components of ground acceleration and velocity (Wald et al. 1999a), Fourier amplitude spectra (FAS, Chernov and Sokolov 1999; Sokolov 2002) or response spectra (Atkinson and Sonley 2000) of horizontal components, or three-component acceleration time histories (JMA instrumental intensity, see http://www.hp1039.jishin.go.jp/eqchreng/at2-4.htm). The instrumental intensity determination is especially useful for the generation of so-called "Shakemaps," which provide information about distribution of damage within a few minutes after a large earthquake (Wald et al. 1999b).

The relationships between seismic intensity and instrumental parameters of ground motion were developed using different databases obtained from earthquakes in various

[a] Geophysical Institute of Karlsruhe University, Herzstr. 16, 76187 Karlsruhe, Germany
[b] Earthquake Research Institute, University of Tokyo, 1-1-1, Yayoi, Bunkyo-ku, Tokyo, Japan

Earthquake Spectra, Volume 24, No. 2, pages 513–532, May 2008;

regions. Thus, there is a necessity for comparative analysis of the relationships to determine potential problems that may occur, for example, when transferring the particular relationship to other regions, or when converting one type of instrumental intensity to another. Atkinson (2001) examined the ability of the relation between response spectra and MM intensity obtained from a Californian database to estimate intensity in eastern North America (ENA) on the basis of available ENA ground-motion relations. Shabestari and Yamazaki (2001) analyzed the relationship between JMA and MM intensities based on three significant earthquakes in California. Sokolov and Wald (2002) compared two methods of instrumental intensity estimation (the peak amplitude technique and FAS-intensity) using data from two relatively recent strong earthquakes: the 1999 (M 7.1) Hector Mine, California, and the 1999 (M 7.6) Chi-Chi, Taiwan.

In this article we analyze the relationship between two techniques for instrumental intensity estimation, namely: the JMA intensity (henceforth denoted by JMA_I) and MM (or MSK) intensity (henceforth denoted by MM_I), which is calculated using the Fourier amplitude spectrum. We used a database that contains records from nine large recent earthquakes in Japan obtained by the high-density strong motion networks of K-NET and KiK-net stations. We selected earthquakes that occurred at different depths and that produced sufficient number of high-amplitude (high-JMA_I) records. The obtained $JMA_I - MM_I$ relationship using a large number of waveform data and from different types of earthquakes in Japan was compared with the same relation obtained recently by Shabestari and Yamazaki (2001) using Californian events.

INPUT DATA

Large recent earthquakes in Japan were chosen for understanding the relation between JMA intensity (JMA_I) and MM intensity (MM_I). The data set includes different types of earthquakes, namely: inland, reverse and strike-slip fault source, intra-plate thrust fault source and inter-plate normal-fault source events occurring in the subducting Pacific plate in northern Japan and in the Philippine-sea plate descending in western Japan.

Ground motions from the earthquakes were recorded by the K-NET and KiK-net nation-wide networks across Japan of over 1800 strong motion instruments which have been deployed across Japan by the National Institute for Earth Science and Disaster Research (NIED) following the destructive damage from the Kobe, Japan earthquake in 1995. The dense strong motion networks cover entirety of Japan at station interval of about 20–25 km. Each seismic station consists of a three-component force-balanced accerograph with a flat response from DC to 30 Hz and a maximum scale of ± 200 cm/s^2; and the data is recorded at a sampling rate of 100 or 200 Hz and a resolution of 24 bit in A/D conversion (Kinoshita 1998; Aoi et al. 2000). The KiK-net stations also have borehole sensors installed on bedrock about 500–3000 m below the surface. The location of earthquake hypocenters used in this study, as well the distribution of K-NET and KiK-net stations are shown in Figure 1. The source parameters of the earthquakes, which are also listed in Table 1, were estimated from a moment tensor inversion using the F-net broadband record of the NIED. Table 2 lists the distribution of the used records versus JMA intensity.

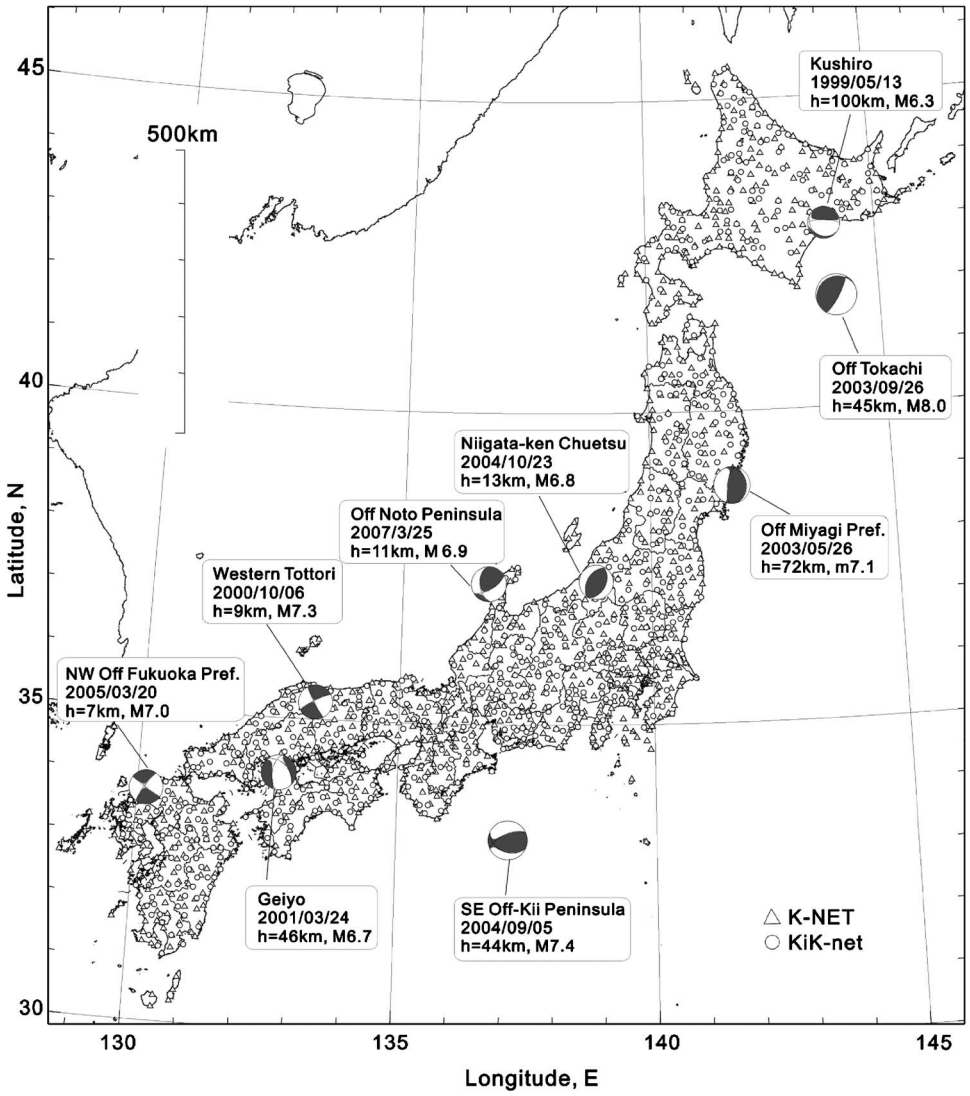

Figure 1. Stations in the K-NET and KiK-net networks across Japan and the epicenters of nine earthquakes used in this study.

DESCRIPTION OF THE TECHNIQUES

JMA INSTRUMENTAL INTENSITY

The previous JMA seismic intensity seven-point scale used in 1949–1996 was defined from felt reports of the strength of ground shaking and damage rates of buildings with most being wooden frame houses. For example, intensity 4 means ground motions most people feel and intensity 5 causing slight damage in buildings such as cracks of

Table 1. Parameters of earthquakes, records from which are used in this study

Event Region	Date & Time (hh:mm, JST)	Location		Magnitude (M_{JMA})	Depth (km)	Mechanism	Number of used records
		N°	E°				
Kushiro region	May 13,1999 02:59	43.0	143.9	6.3	100	Normal fault (inter plate)	116
Western Tottori Pref.	Oct. 6, 2000 13:30	35.3	133.4	7.3	9	Strike-slip (intra plate)	106
Geiyo	Mar. 24, 2001 15:27	34.1	132.7	6.7	46	Normal fault (inter plate)	119
Off Myagi Pref.	May 26, 2003 18:24	38.8	141.8	7.1	72	Normal fault (inter plate)	188
Off Tokachi	Sept. 26, 2003 04:50	41.85	143.77	8.0	45	Thrust (inter plate)	415
Niigata-ken Chuetsu	Oct. 23, 2004 17:56	37.3	138.77	6.8	13	Reverse fault (intra plate)	339
SE Off Kii Peninsula	Sept. 5, 2004 23:57	33.2	137.1	7.4	44	Thrust (inter plate)	358
NW Off Fukuoka Pref.	Mar. 20, 2005 10:53	33.85	129.98	7.0	7	Strike-slip (intra plate)	250
Off Noto Peninsula	Mar. 25, 2007 9:41	37.22	136.69	6.9	11	Reverse fault (intra plate)	95

wall, as well as the collapse of grave stones and stone lanterns. During intensity 6, most people are unable to keep standing and collapse is caused to about 30% or less wooden frame buildings. The largest intensity 7 means more than 30%–50% of wooden frame houses collapse. Following the Kobe earthquake in 1995 an instrumental intensity scale

Table 2. Distribution of records versus JMA intensity (>2)

JMA intensity scale	Instrumental intensity (JMA_I) ranges	Total
2	$2.0 \le I < 2.5$	559
3	$2.5 \le I < 3.5$	829
4	$3.5 \le I < 4.5$	420
5−	$4.5 \le I < 5.0$	86
5+	$5.0 \le I < 5.5$	65
6−	$5.5 \le I < 6.0$	20
6+	$6.0 \le I < 6.5$	5
7	$6.5 \le I$	2

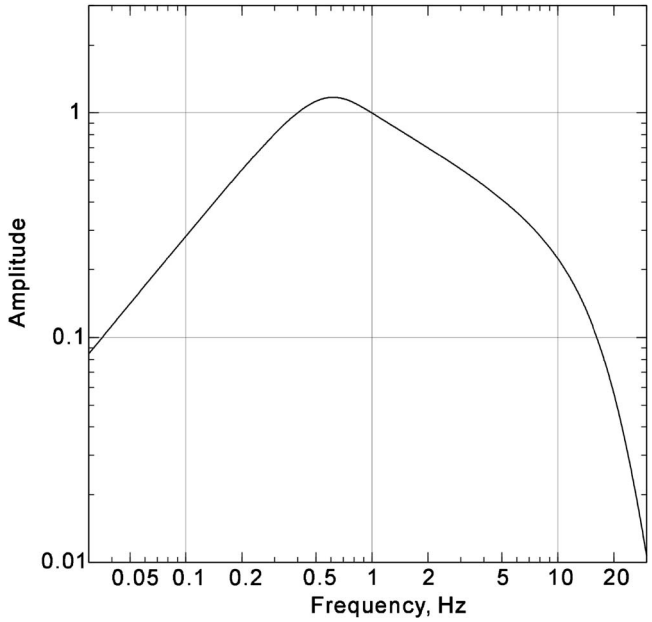

Figure 2. Response curve of a band-pass filter used for estimating the JMA instrumental intensity.

is introduced in the existing JMS intensity enabling rapid estimation of the strength of ground motion and the resulting damage caused by large earthquakes (see http://www.hp1039.jishin.go.jp/eqchreng/at2-4.htm).

The modern intensity measurement system basically follows the traditional JMA intensity scale and the intensity is automatically estimated using three-component ground acceleration records after applying a band-pass filter as shown in Figure 2. The frequency response characteristics of this band-pass filter emphasize felt strength of the ground shaking around 0.5 Hz which is also related to the damage of wooden frame houses in Japan during large earthquakes. Also, the strong cut-off in high-frequency signals of over about 10 Hz means that high-frequency ground acceleration of frequency in this range is completely ignored during the intensity estimation.

The estimation procedure of the JMA intensity scale is as follows (see also Shabestari and Yamazaki 2001). Fourier transform is applied for each of three-component acceleration time history. Then the band-pass filter is applied in the frequency domain. After transforming back into the time history, the square root of vectoral composition of the three components in time domain is used for calculation of cumulative duration τ as a function of acceleration amplitude (Figure 3). The cumulative duration is the total time duration exceeding given value of the vectoral acceleration. Then, the maximum amplitude a_0 of the vector composition is examined. During this procedure a_0 must satisfy

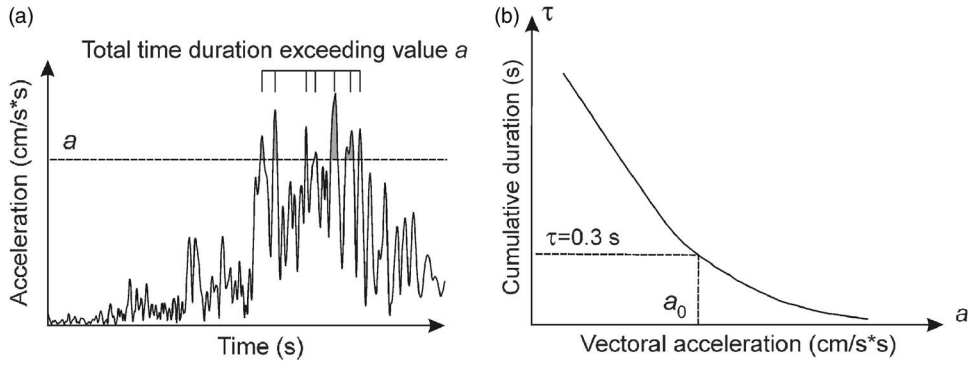

Figure 3. Estimation of JMA intensity (see text). (a) Calculation of cumulative duration τ from vectoral composition of accelerogram. (b) Evaluation of a_0 value used for calculation of the instrumental JMA intensity.

cumulative duration over 0.3 s, and, therefore, transient large accelerations such as spiky signals with duration less than 0.3 s are omitted. Finally the JMA intensity (JMA_I) is obtained using the following equation:

$$JMA_I = 2\log(a_0) + 0.94 \tag{1}$$

The relation between JMA intensity scale and JMA instrumental intensity ranges is shown in Table 2.

FAS (FOURIER AMPLITUDE SPECTRUM) INTENSITY

It has been found that the seismic intensity is determined by the level of ground motion (amplitudes of FAS) in the frequency range of 0.4–13 Hz (Chernov 1989; Chernov and Sokolov 1999; Sokolov 2002; Sokolov and Wald 2002). The details of the analysis, which is based on a large number of earthquake records obtained in various seismic regions and corresponding observed macroseismic intensity values, may be found in the above mentioned papers. Here we describe shortly the concept of the FAS intensity.

When studying the relationship between seismic intensity I (MM or MSK scales) and the Fourier amplitude spectrum of ground acceleration A, the distribution of the FAS values at different frequencies is analyzed for various intensities (IV–IX). The differences in earthquake parameters (magnitude, source mechanism, and distance), regional tectonics, propagation path properties, recording sites, and geological and geotechnical conditions are not taken into account. These factors are considered as random variables affecting the ground motion parameters for a given intensity level. It has been found that the variances (or standard deviations) of the distribution of $\log A$ values are not the same at different frequencies. It is reasonable to suggest that the contribution of ground motion components to the ground motion severity varies with frequency and that the variances are the least at the frequencies that are most "representative" for a given intensity level.

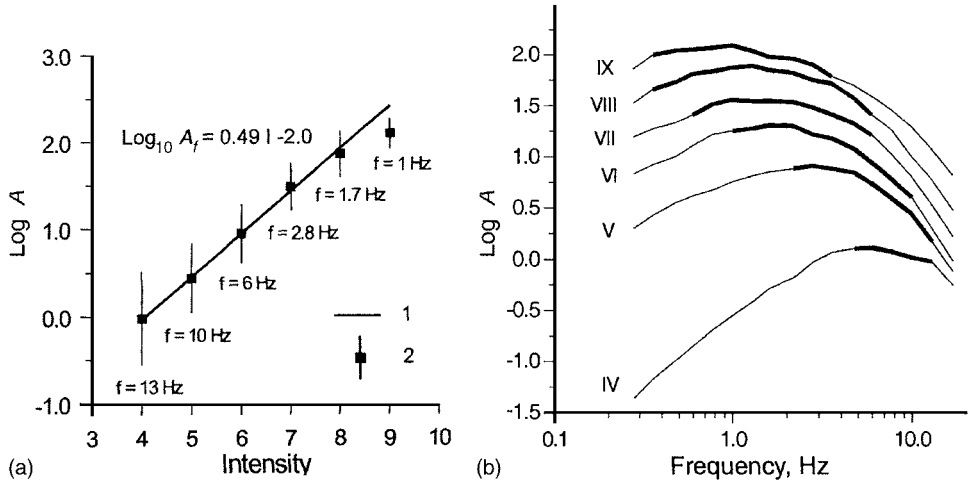

Figure 4. Fourier acceleration spectra/intensity relationship. (a) Linear regression for "representative" frequencies (1); mean±one standard deviation of the data (2). (b) Mean acceleration spectra (cm/s) for different intensities (IV–IX MMI). Thick lines show spectral amplitudes located within the "representative" frequency ranges.

The correlations between the values of $\log A$ and the levels of intensity I were studied for all possible combinations of considered frequencies and intensities. The linear regression $\log A = F(I,f)$, which is characterized by the largest correlation coefficient $R = 0.86$, is shown in Figure 4a. The values of $\log A$ in this correlation are determined at the "representative" frequencies f_R, which depend on the intensity and decrease with increasing intensity level. In reality, the intensity of ground shaking is determined by the joint influence of ground-motion components at different frequencies; however, the contributions of these components change with frequency. Figure 4b shows the average spectra for different intensities and the parts of the spectra located within the "representative" frequency ranges. The "representative" portions become wider (in terms of logarithm of frequency) and move to the low-frequency part of the spectra with increasing intensity.

The spectral amplitudes should be considered as random variables and appear to be lognormally distributed. Thus, in order to estimate the intensity level I, it is necessary to calculate probability distribution function $F(i) = P[I \leq i]$, where i is the value of I in the range of interest. The desired value of instrumental intensity is estimated by the maximum of the first derivative of function P. The scheme of calculation has been described in Sokolov (2002) and Sokolov and Wald (2002).

The concept of the FAS intensity may be interpreted as follows. The damage potential of ground shaking depends on amplitude, duration and frequency content of the motion. The descriptive macroseismic scales use typical indicators that characterize the earthquake influence. For small intensities these indicators are associated with high-frequency vibrations (human fear, disturbance of dishes, windows and doors, falling of

small unstable objects). The second group of indicators is considered for increased level of ground motion, namely: damage of construction and their components. These effects are caused by intermediate-frequency vibrations (in the considered range of 0.3 Hz – 12 Hz). Finally, the largest macroseismic effects of the earthquake (landslides and relief changes) result from intensive long-period seismic vibration. These phenomena, as revealed from instrumental records, may also cause such long-period vibration themselves.

The increase in the severity of shaking (or intensity) in the middle part of macroseismic scale should be accompanied by quantitative changes in response of construction. Relatively small intensities (less than MM VII) are characterized by damage of "small parts" of structures (cracks in walls, chimneys, etc.) that are caused by short-period vibrations. Greater damage (MM VII–VIII) is characterized by collapse of panel and brick walls, spans and ceilings, falling of heavy furniture. Damaged structures completely collapse (MM > IX) because of the influence of both (1) short- and intermediate-period components of vibration, and (2) sufficiently intensive long-period motions. Thus, the growth of macroseismic effects in range of MM VI–IX may be interpreted as follows. Continuously growing effects are caused by increased amplitudes of relatively high-frequency vibrations. The natural frequency of partly damaged structure decreases and, when the amplitudes of longer-period motion reach a certain level, there should be a change of structural response to a higher level of macroseismic effect. Thus, to cause a higher level of damage, besides a sufficient level of relatively long-period vibration, there should also be a "sufficient" amount of high-frequency components. The procedure of intensity estimation from the Fourier Amplitude Spectrum takes into account these phenomena through widening of "representative" frequency range and the increase in the level of spectral amplitudes at these frequencies.

RESULTS AND DISCUSSION

REGRESSION PROCEDURES

We estimate the parameters of a function that relate two variables using the least squares technique (Rawlings et al. 1998). Several implicit requirements should be accepted in this case. In so-called ordinary least squares (OLS) we should assume that the independent (predictor) variables are measured without error and all the errors are in the dependent (response) variables. In this study we analyze instrumental intensity and we do not consider its relation to macroseismic (observed) intensity. The instrumental intensity values are determined using simple mathematical procedures from ground motion records. Thus, if we consider the instrumental intensity as a characteristic of a given ground motion recorded at a specific site, we can accept the requirement of non-error predictor. The errors in response variable, in this case, are caused by application of different technique of instrumental intensity estimation. For example, the influence of vertical component is not taken into account in the FAS technique. Also, as can be shown later, the frequency content of ground motion can significantly affect the correlation between instrumental intensity values.

However, when relating the calculated instrumental intensity values to earthquake effect within an area, it is necessary to consider possible variations of ground motion field within the area. The variability may be very large even over distance of tens or hundreds of meters. The standard regression procedures based on OLS technique, in which the uncertainty of the predictor variable is assumed to be relatively small, are not applicable for this case. The so-called *orthogonal regression*, in which the model errors are distributed over the predictor and response variables, should be used to determine linear relationships between two types of instrumental intensity. The technique, which is also called as *total least squares* (TLS), minimizes the sum of the squared perpendicular distances from the data point to a line.

However, we have one more problem – the analyzed data are unbalanced and they seem to be heteroscedastic, i.e. the variables apparently have different variances. One of the simplest ways to correct for the effect of imbalanced data is application of so-called *unweighted analysis of cell means* (UWCM). Another technique, which is also applied to treat heteroscedasticity, is to use the *weighted least squares* scheme. As a rule, weights are given as the inverse of variance, giving point with lower variance a greater statistical weight. However, should we apply greater weights to large intensity points because there is only a few observations (and lower variance), or because the large intensity range is of great importance? When the weights are estimated using only a few observations, the results of an analysis can be unpredictable affected. Therefore we assumed that each observation, even the apparent outlier, brings an equal contribution to the final parameter estimates.

Obviously, this apparent imbalance is caused by a large difference among the sizes of the observations. Large earthquakes produce much more small and intermediate intensity records than that for large intensities. We will never get an equal number of observations for every range of intensity without artificial sampling from small and intermediate intensities. The heteroscedasticity is an inherent peculiarity of such types of data. Another reason for the heteroscadasticity in the considered instrumental intensities relation will be discussed later.

In our analysis we used the OLS technique including unweighted analysis of cell means and orthogonal regression technique.

RELATIONSHIP BETWEEN INSTRUMENTAL INTENSITIES

The distribution of MM_I versus JMA_I (and vice versa) based on the data used in this study is shown in Figure 5. It seems that the relation is not linear for the whole considered dataset. We can divide the data into two distinct intervals with the linear relationships, namely: below and above JMA_I 3.5.

The reason for the difference between the considered types of instrumental intensities may be explained as follows. The "representative frequencies" for small intensity records belong to relatively high-frequency part (about 8–9 Hz, see Figure 4), however such high-frequency components are not used in the evaluation of the JMA_I. Therefore,

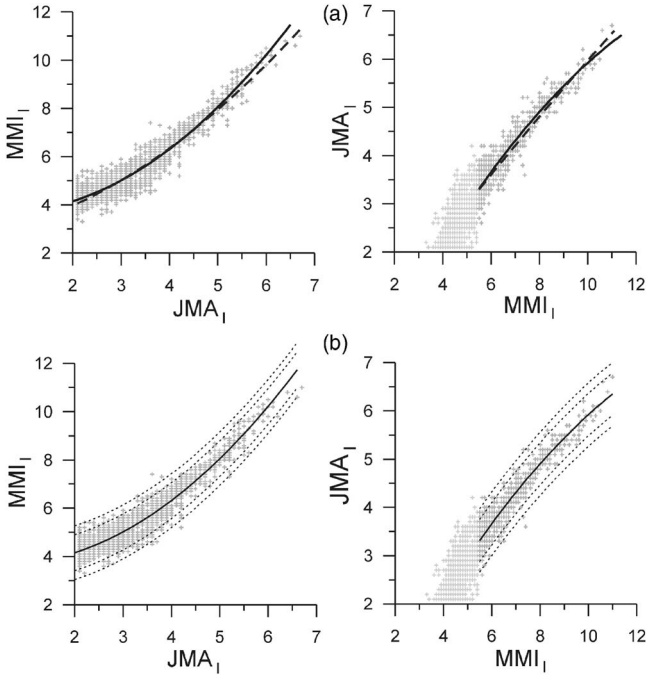

Figure 5. Distribution of JMA_I versus MM_I and vice versa. (a) Nonlinear (quadratic) relationships. solid lines – OLS technique, all data; dashed lines - UWCL technique, all data. (b) Nonlinear relationships obtained using OLS technique (solid lines) and ±2 and 3 standard error limits (dashed lines). Dark gray symbols denote the data used for developing of the relationships.

in the small intensity range the increase of JMA_I values is not accompanied by the corresponding increase of MM_I values until the FAS "representative frequencies" become close to frequency range used for estimation of JMA_I (Figure 2).

The quadratic MM_I–JMA_I relationship for the whole dataset and JMA_I–MM_I relationship for $MM_I > 5.5$ evaluated using OLS technique are described as

$$MM_I = 3.737(\pm 0.109) - 0.228(\pm 0.063) \times JMA_I + 0.218(\pm 0.009) \times JMA_I^2 \quad [0.371] \tag{2}$$

$$JMA_I = -1.434(\pm 0.296) + 1.019(\pm 0.081) \times MM_I - 0.028(\pm 0.005) \times MM_I^2 \quad [0.219] \tag{2a}$$

where the values in parenthesis denote the standard errors of coefficients, and the values in square brackets denote standard error of regression. The similar relationships evaluated using UWCM technique are as follows:

$$MM_I = 2.646(\pm 0.377) + 0.391(\pm 0.184) \times JMA_I + 0.134(\pm 0.021) \times JMA_I^2 \quad (3)$$

$$JMA_I = -0.271(\pm 0.015) + 0.679(\pm 0.004) \times MM_I - 0.005(\pm 0.0002) \times MM_I^2 \quad (3a)$$

It seems that the OLS fit is governed by the small and moderate intensity values. The instrumental intensity values may be overestimated for the case of MM_I–JMA_I relation, or underestimated for the case of JMA_I–MM_I, relation when being calculated using equations from high values of the predictor. However, we have only three observed values in this intensity range and the difference between the observations and the model can not be considered as significant.

Let us consider the upper part ($JMA_I > 3.5$; $MM_I > 5.5$), which is of particular interest for earthquake engineering applications. The OLS estimations of linear relations are

$$MM_I = -0.584(\pm 0.107) + 1.743(\pm 0.024) \times JMA_I \quad [0.384], \quad R = 0.94 \quad (4)$$

$$JMA_I = 0.105(\pm 0.052) + 0.595(\pm 0.008) \times MM_I \quad [0.224], \quad R = 0.95 \quad (4a)$$

where R is the correlation coefficient. The similar relationships evaluated using UWCM technique are as follows:

$$MM_I = -0.634(\pm 0.273) + 1.74(\pm 0.052) \times JMA_I \quad (5)$$

$$JMA_I = 0.278(\pm 0.112) + 0.568(\pm 0.013) \times MM_I \quad (5a)$$

Figure 6a shows the linear relationships (OLS case) and standard error limits. The UWCM technique produces the similar result.

Let us consider errors in the calculated instrumental intensity values, both in the predictor and the response variables. The orthogonal regression requires knowledge of the error variance ratio $\eta = \sigma_\varepsilon^2 / \sigma_u^2$, where σ_ε^2 is the error in the response variable and σ_u^2 is the error in the predictor. We assume that the errors are equal in terms of units of considered intensity scales, i.e. $\eta = 12/7$ for MM_I–JMA_I relation and $\eta = 7/12$ for JMA_I–MM_I relation.

The technique of orthogonal regression uses perpendicular distances from the data point to a straight line. Therefore, when selecting the data set for analysis, we can not simply take all data, the x-coordinate of which is larger than a certain value (e.g. $JMA_I > 3.5$) like we did in the previous cases. We do not know, from the beginning, parameters of the line and the following iteration procedure is applied. First, the regression coefficients a and b were evaluated using all data, for which $JMA_I > 3.5$. Then, we select all data (x_1, y_1), the projection of which on the regression line (x_0, y_0) satisfy the relation $x_0 > 3.5$ $[x_0 = (by_1 + x_1 - ba)/(b^2 + 1)]$. The new regression coefficients are evaluated and the procedure is being applied again until the difference between the numbers of data points of two consecutive iterations become negligible.

When applying the orthogonal linear regression technique for MM_I–JMA_I relationship, the following equation has been obtained for $JMA_I > 3.5$ and $MM_I > 5.5$:

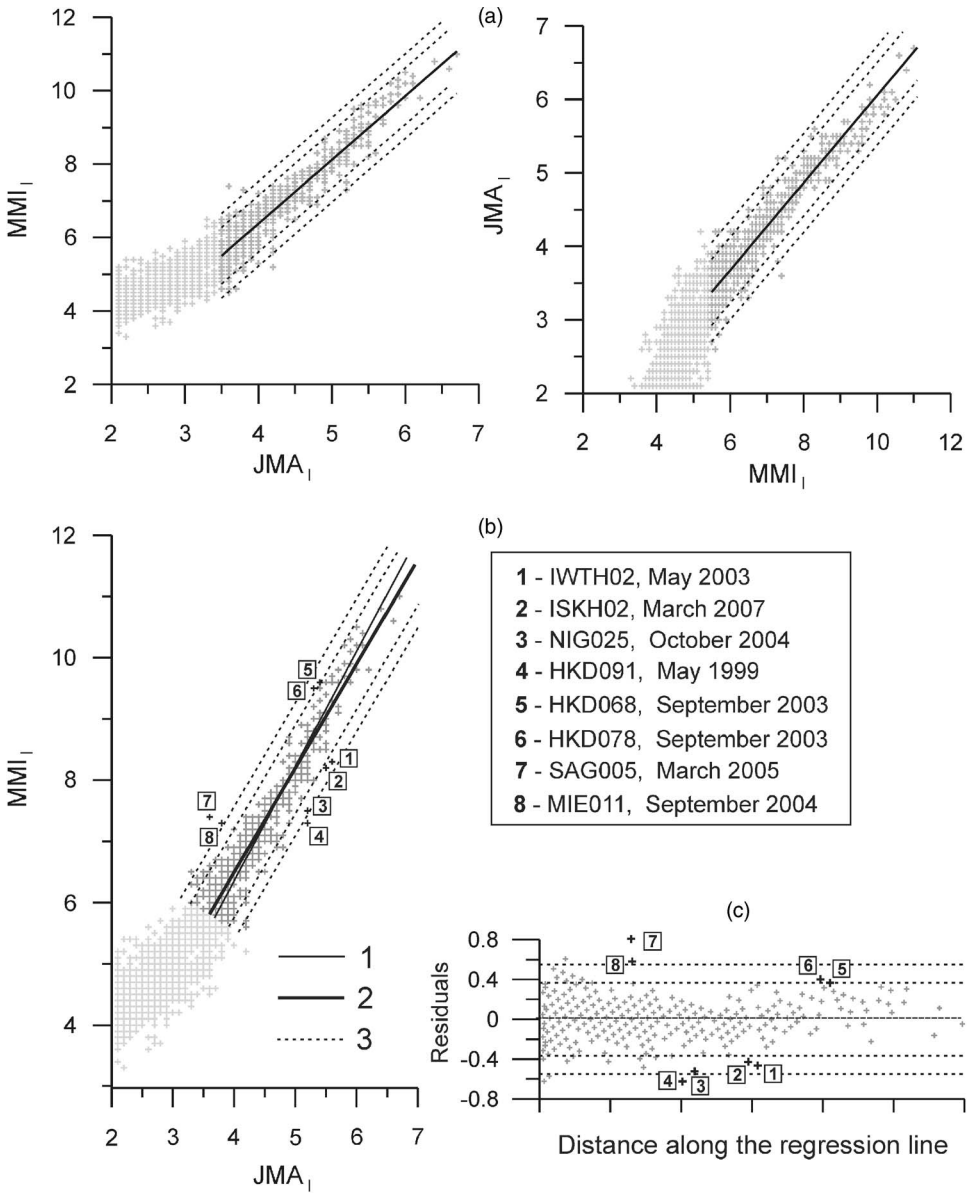

Figure 6. Linear relationships between JMA_I and MM_I and vice versa. (a) The ordinary least squares technique (eqs. 4 and 4a); dashed lines show ±2 and 3 standard error limits. Dark gray symbols denote the data used for developing of the relationships. (b) The orthogonal regression technique. Solid lines: 1 – linear relationship evaluated after the first step of iteration ($JMA_I > 3.5$, see text); 2 – final estimation (eq. 6). Dashed lines show ±2 and 3 standard error limits. The selected extreme cases are marked (station and earthquake). (c) Distribution of residuals calculated as difference between the particular instrumental intensity values and the correspondent linear relationship (Equation 6). Dashed lines show ±2 and 3 standard error limits.

$$MM_I = -0.32(\pm 0.107) + 1.703(\pm 0.024) \times JMA_I \quad [0.188] \tag{6}$$

$$JMA_I = 0.189(\pm 0.050) + 0.585(\pm 0.007) \times MM_I \quad [0.186] \tag{6a}$$

Figure 6b shows the linear relationships for the orthogonal regression case and standard error limits. The standard error of regression is a measure of misfit between the observations and the used model. If the uncertainties are related to the predictor and response variables, the model error σ_M can be treated as follows. Suppose that a certain value of JMA_I instrumental intensity was calculated from a given record. Thus, assuming normal distribution of the intensity values and the error variance ratio η accepted above, we can expect that with probability 99.5% the possible values of JMA_I would lie within the following limits: $JMA_I \pm 3\sigma_M \sin(90° - \alpha)$; $\alpha = arctg(b)$, where b is the slope of regression line. The correspondent values of limits for the MM_I instrumental intensity can be calculated using Equation 6. For example, for $JMA_I = 5.0$ the limits are 4.5–5.5, and the MM_I limits are 7.4–9.0. However this standard error value has been evaluated for the whole dataset used for estimation of the regression. Different intervals of the intensity, most likely, will be characterized by various standard error values.

Figure 6c show characteristics of scatter calculated as distance between particular instrumental intensity pairs and the correspondent linear relationship. In some cases the residual can exceed a value of $2\sigma_M$ or even $3\sigma_M$. What is a reason for such scatter? We selected a few extreme cases (records), which are characterized by the highest residuals. The records are marked in Figure 6b and 6c by the name of station and earthquake. Figure 7 shows examples of time histories and spectra for some of the marked records. The values of instrumental intensity (JMA_I and MM_I), as well as the residuals, are given in Table 3.

It is obvious that the scatter relates to spectral content of ground motion. The JMA instrumental intensity is evaluated from filtered three-component accelerograms. This band-pass filter is characterized by maximum amplitude at frequencies of 0.5 Hz (Figure 2). Thus, the procedure of JMA calculation is sensitive to sharp peaks of spectral amplitudes around this frequency range. The cases of spectra with high-amplitude narrow-band peaks (e.g. IWTH02, May 2003; NIG025, October 2004) or records with predominant frequencies about 0.5–2.0 Hz (e.g. ISKH02, March 2007; HKD091, May 1999) are associated with higher than average values of JMA_I. The most prominent difference (residual about 0.52) was obtained for station NIG025, which is characterized by narrow-band peak at about 1.8 Hz and relatively small amplitudes of the high-frequency components of ground motion. The record obtained at station IWTH02 has low frequency content within the range of 0.5–2.0 Hz, which are the frequencies privileged by JMA_I. However, due to a strong site amplification effect, the spike at 5 Hz is very high (about 70–80 times larger than at about 2–3 Hz), that is sufficient to contribute significantly to JMA_I.

The influence of the high-amplitude vertical component of ground motion for stations IWTH02 and ISKH02 on the discrepancy between the JMA_I and MM_I values can not be considered as significant due to the frequency content of vertical component. We calculated the JMA_I values for these records reducing the amplitudes of vertical com-

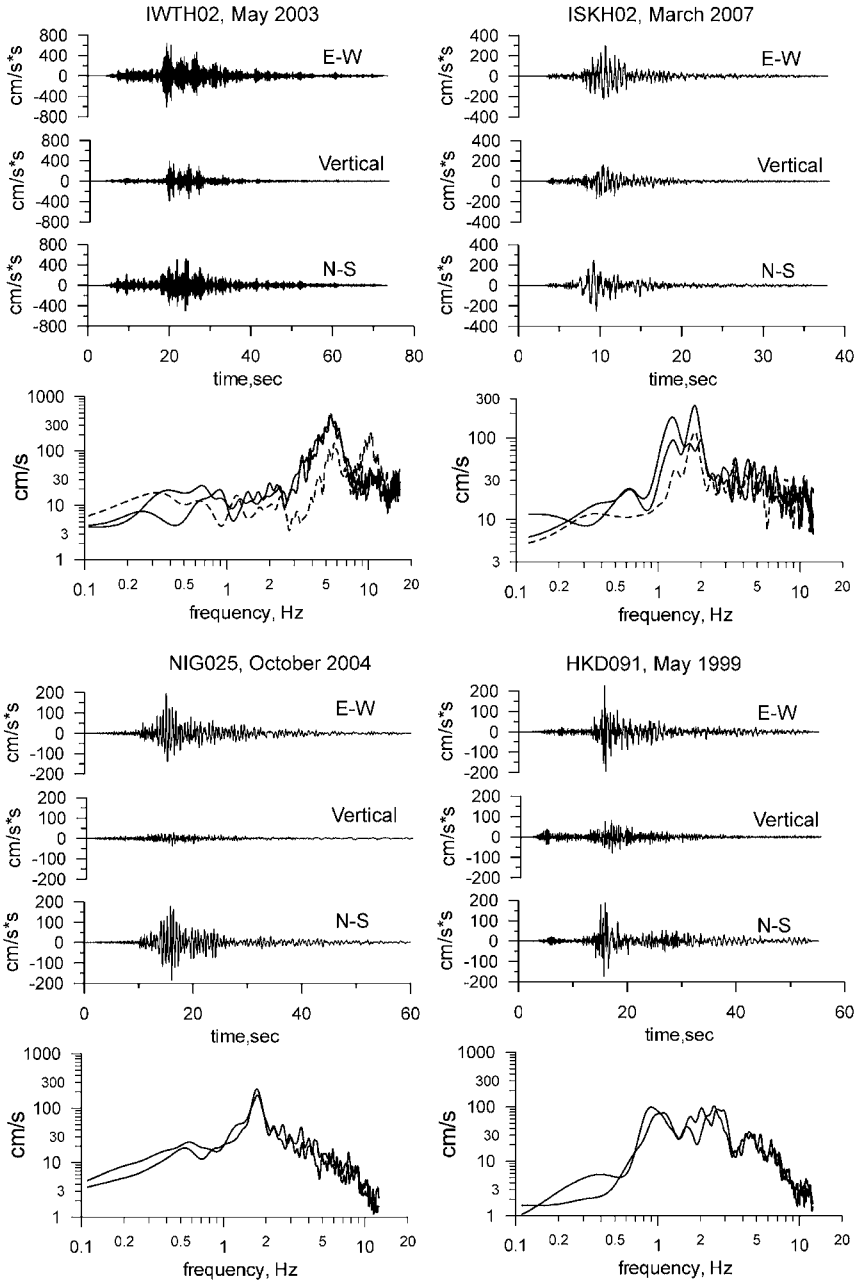

Figure 7. Acceleration records and Fourier Amplitude spectra for the cases shown in Figure 6. Solid lines show spectra of horizontal components; dashed lines–spectra of vertical components.

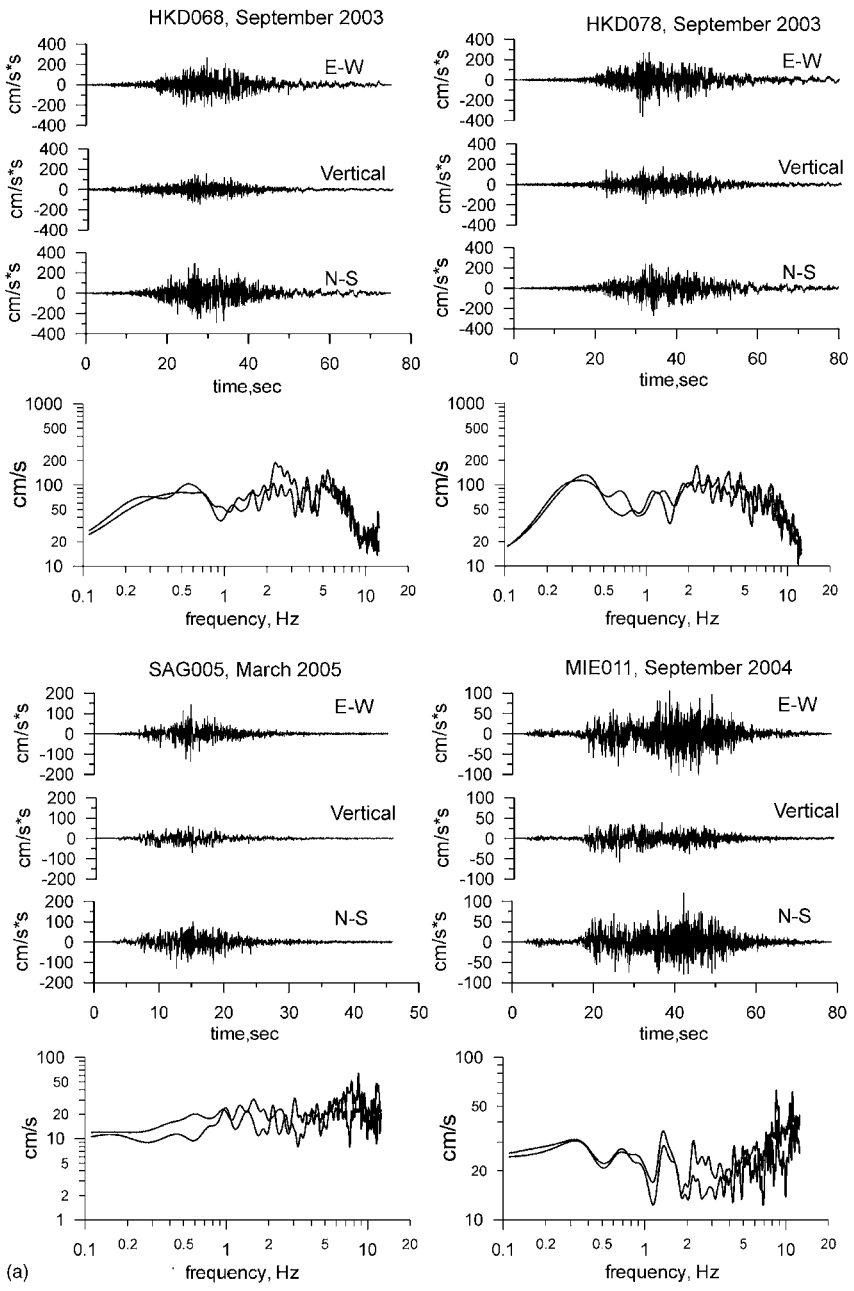

Figure 7. (cont.)

Table 3. Characteristics of extreme cases (records) marked in Figure 6. Values in parentheses show difference (residuals) between the calculated values of instrumental intensity and estimations from the corresponding regression (see Figure 6b)

Station Code	Event Name	Labelling in Figure 6	Epicentral Distance (km)	$JMA_I - MM_I$
IWTH02	Off Myagi Pref.	1 (May 2003)	120	5.6–8.3 (−0.46)
ISKH02	West coast of Honshu	2 (March 2007)	35	5.5–8.1 (−0.43)
NIG025	SE Off Kii Peninsula	3 (October 2004)	55	5.3–7.3 (−0.48)
HKD091	Kushiro region	4 (May 1999)	105	5.2–7.5 (−0.52)
HKD068	Off Tokachi	5 (September 2003)	170	5.4–9.6 (0.36)
HKD078	Off Tokachi	6 (September 2003)	160	5.3–9.5 (0.32)
SAG005	NW Off Fukuoka Pref.	7 (March 2005)	50	3.8–7.3 (0.59)
MIE011	SE Off Kii Peninsula	8 (September 2004)	165	3.6–7.4 (0.80)

ponent by 100 times and the received values are less than the normal ones by 0.1 units of JMA for station IWTH01 and 0.2 units of JMA for station ISKH02.

The broad-band (HKD068 and HKD078, September 2003; SAG005, March 2005) and high-frequency vibrations (MIE011, September 2004) produce smaller, than average, JMA_I values, but higher than average MM_I values. The most prominent difference (residual about 0.80) was obtained for station MIE011, which is characterized by relatively low-amplitude components of ground motion within the frequency range 0.5–3.0 Hz. The same phenomenon caused large $JMA_I - MM_I$ discrepancy for records obtained at stations HKD068 and HKD078.

We should note, that the influence of high-frequency components on MM_I estimations can be important not only for low intensities, for which the most "representative" portions of the spectra belong to frequencies more than 3–4 Hz. Intensities of $MM_I > VII–VIII$ represent majority of motions that cause the damage to buildings and their components, brittle and flexible, which are sensitive to various frequencies of vibration. Thus, the relatively high value of MM_I intensity evaluated from the broad-band records (e.g. SAG005) reflects overall damage of various structures and buildings of different height, not only damage of traditional wooden frame houses. On other hand, the high-amplitude but narrow-band vibrations could produce strong resonance effects for a particular structure; however that vibration can hardly cause the overall damage, which should be assigned to high intensity level. The record obtained at station NIG025, the spectra of which are characterized by a high, but narrow-band amplitudes, can be considered as an example.

Bearing in mind the dependence of the $MM_I - JMA_I$ relation on the spectral content

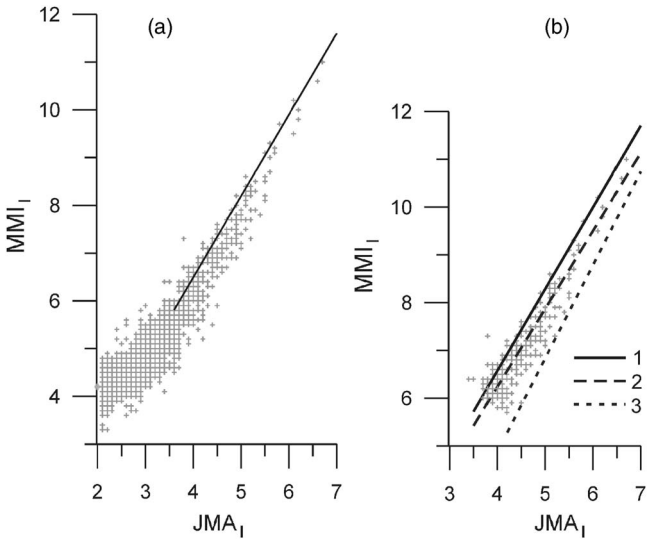

Figure 8. Comparison between JMA_I–MM_I relations obtained in for various earthquakes. (a) The generalized linear relationship (Equation 6) and distribution of JMA_I–MM_I pairs for intermediate magnitude shallow inland earthquakes in Japan. (b) The JMA_I–MM_I relations evaluated for two sets of data: subduction (1) and inland earthquakes (2) in Japan, and the relationship presented by Shabestari and Yamazaki (2001) based on Californian earthquakes (3).

of ground motion, it is easy to explain the apparent division of the relation into two parts below and above of JMA_I 3.5 (MM_I 5.5–6.0, see Figures 5 and 6). The representative portion of spectrum for MM_I intensities less than VI is located above frequencies of 1.0–2.0 Hz. Thus, the JMA_I and MM_I values for relatively small intensities are determined using different parts of spectrum. Our database contains records from large earthquakes and small intensities are associated with long-distant vibrations, which are characterized by intensive long-period motions and by "lack" of high-frequency amplitudes. The influence of thin superficial layers below particular stations or the propagation path for particular earthquakes (Furumura and Kennett, 2005), which adds the high-frequency signals to the motion, in this range of intensities lead to especially high scatter of JMA_I for approximately same values of MM_I.

The database used in our study contains records from large earthquakes of various focal mechanisms, which occurred in different depths and regions of Japan. We also compiled a dataset containing records from 19 intermediate magnitude (M 5.5–6.5) shallow inland earthquakes, which occurred during the period of 2004–2007. The MM_I–JMA_I distribution for this dataset and the generalized MM_I–JMA_I relation obtained for the large earthquakes (Equation 6) are shown in Figure 8a. The dataset shows higher, than average, JMA_I values, but smaller, than average, MM_I values. We also selected two groups of data, namely: (a) subduction zone events (2003 Off Tokachi, 2003 Off Miyagi, and 2004 Off Kii) and (b) inland events (2004 Chuetsu, 2000 Tottori, 2003

Fukuoka, 2007 Honshu, and 19 intermediate magnitude events). Figure 8b shows correspondent $JMA_I - MM_I$ relations for $JMA_I > 3.8$ and distribution of the data from shallow inland earthquakes. Despite the scatter of the particular observations it is possible to conclude that the inland earthquakes represent a so-called *small MM_I - high JMA* (*SM-HJ*) tendency, while the subduction earthquakes producing relatively high-frequency radiation may be called as *high MM_I—small JMA* (*HM-SJ*) events.

When applying the orthogonal linear regression technique, the following equation has been obtained for the subduction zone events and inland events ($JMA_I > 3.8$)

$$MM_I = -0.265(\pm 0.128) + 1.71(\pm 0.029) \times JMA_I \quad [0.186] \quad \text{subduction events} \quad (7)$$

$$MM_I = -0.295(\pm 0.153) + 1.633(\pm 0.035) \times JMA_I \quad [0.182] \quad \text{inland events} \quad (7a)$$

However, the apparent difference between the data sets collected during the large earthquakes may be caused by peculiarities of the available database, for example, influence of local site conditions. Ideally, for robust and confident conclusions to be drawn regarding the influence of characteristics of earthquake source zone and propagation path on the $MM_I - JMA_I$ relation the datasets for inland and subduction events should contain records obtained at the same stations and the same epicentral distances.

Recently Shabestari and Yamazaki (2001) analyzed relations between instrumental JMA (JMA_I), observed (MM_O), and instrumental (MM_I) intensity for three recent earthquakes in California. Figure 8b compares our relationships between JMA_I and MM_I and the JMA_I and MM_O relationship obtained by Shabestari and Yamazaki (SY).

The SY relationship gives smaller MM intensity values for the same JMA intensity than that in our relationships. On one hand, the phenomenon agrees with conclusions made in a recent paper (Sokolov and Wald 2002) after comparison between two techniques of instrumental intensity evaluation. One of the techniques is based on Fourier amplitude spectra (FAS) and the other–on peak amplitudes of acceleration and velocity (Wald et al. 1999a) developed for California. The direct comparison of the techniques showed that the FAS method, which is based on worldwide data and therefore averages different building codes and quality of construction, resulted in the higher MM_I values than the peak amplitude technique.

The peak amplitude-based relationship characterizes existing building stock in California constructed in accordance with stronger building code. Thus, the relationship of Wald et al. (1999a) provides lower intensity levels for the same peak motions than relationships developed before. We can conclude that both considered $MM_I - JMA_I$ relations are reliable – our relation describes the worst (pessimistic) case and the Shabestari and Yamazaki relation, which reflects improved building practices in California, gives the optimistic variant. We should note, however, that Shabestari and Yamazaki (2001) used a few data with limited MM_O (MM_I) range from 4–8 and the obtained $JMA_I - MM_I$ relation reveals very large scatter.

On other hand, the difference between the relations obtained in this study and those proposed by Shabestari and Yamazaki may be also explained by peculiarities in the frequency content of ground motion, which depends on effects of source, propagation path

and local site conditions. In some cases, the influence of the particular factor may be predominant; in the others, the joint influence of the factors determines the shape and level of ground motion spectra. Some KiK-net stations in Japan are located at rock sites covered by very thin superficial layers. Such layer causes strong site amplification in a high-frequency band over 5–10 Hz. It has been also shown by Furumura and Kennett (2005) that the subducting plate is an efficient waveguide of very high-frequency signals. The net effect of propagation path and site amplification produces anomalously large ground accelerations with very high-frequency signals during subduction zone earthquakes occurring the Pacific plate in NE Japan. In contrast, the PGA in California is carried by lower-frequency motions due to greater high-frequency attenuation. Therefore, the shallow earthquakes in California belong to *small MM_I-high JMA_I* events.

CONCLUSION

The relation between two types of instrumental intensity (JMA_I and spectral MM_I), as has been found from analysis of records obtained during recent strong earthquakes in Japan, may be described as linear function in large intensities range over about 3.5 for JMA_I and 5.5–6.0 for MM_I. However, the relationship is characterized by a remarkable degree of scatter. The variation is most probably caused by differences in the spectral content of the ground motions considered in each method. It seems that the relationships are different for the subduction and shallow inland earthquakes.

The $JMA_I - MM_I$ relation, which was estimated in this study, differs from a simple linear $JMA_I - MM_I$ relation (applied for wide intensity range between $2 < JMA_I < 7$) obtained by Shabestari and Yamazaki (2001) from the data of three Californian earthquakes. The Shabestari and Yamazaki relationship gives higher JMA_I values for the same MM_I than that predicted from our relationships. The phenomenon agrees with conclusions made in a recent paper (Sokolov and Wald 2002) after comparison between two techniques of instrumental intensity evaluation. The Shabestari and Yamazaki relation reflects improved building practices accepted in California. The spectra-based technique of instrumental intensity calculation was developed using worldwide data and therefore it averages different building codes and quality of construction.

Besides the improved building practices, the difference may reflect influence of earthquake characteristics (focal mechanism, peculiarities of the rupture propagation and slip distribution), properties of propagation path and local geological conditions. Bearing in mind the dependence of the $JMA_I - MM_I$ relation on spectral content of ground motion, we can suggest that thrust events, which occurred within rigid platform and recorded mainly at rock sites (e.g. North-Eastern America, or Canada), would provide different $JMA_I - MM_I$ relationships than strike-slip events occurring in California and recorded mostly at soft soil sites. The last case would be characterized by *high JMA_I–small MM_I* relation. Thus, care should be taken when comparing the man-felt area and the distribution of intensity contours for the Japanese earthquakes defined by JMA_I and others described by MM_I.

ACKNOWLEDGMENTS

The authors would like to thank Peter Stafford for thoughtful review comments and suggestions, which significantly helped to improve the earliest version of the article. The constructive comments from anonymous reviewers are gratefully acknowledged. We thank to the National Institute for Earth Science and Disaster Research, Japan for providing K-NET and KiK-net data.

REFERENCES

Aoi, A., Obara, S., Hori, S., Kasahara, K., and Okada, Y., 2000. New strong observation network KiK-net, *EOS Trans. Am. Geophys. Union* **81**, F863.

Atkinson, G. M., 2001. An alternative to stochastic ground-motion relations for use in seismic hazard analysis in Eastern North America, *Seismol. Res. Lett.* **72**, 299–306.

Atkinson, G. M., and Sonley, E., 2000. Empirical relationships between Modified Mercalli intensity and response spectra, *Bull. Seismol. Soc. Am.* **90**, 537–544.

Chernov, Y. K., 1989. *Strong ground motion and quantitative assessment of seismic hazard*, Fan Publishing House, Tashkent, 296 pp. (in Russian).

Chernov, Yu. K., and Sokolov, V. Yu., 1999. Correlation of seismic intensity with Fourier acceleration spectra, *Physics and Chemistry of the Earth, Part A: Solid Earth and Geodesy*, 24(6), 522–528.

Furumura, T., and Kennett, B. L. N., 2005. Subduction zone guided waves and the heterogeneity structure of the subducted plate: intensity anomalies in northern Japan, *J. Geophys. Res.* **110**, B10302. , 1–27.

Kinoshita, S., 1998. Kyoshin Net (K-NET), *Seismol. Res. Lett.* **69**, 309–332.

Rawlings, Jh. O., Pantula, S. G., and Dickey, D. A., 1998. *Applied regression analysis: a research tool*. Springer, New York, 658 pp.

Shabestari, Kh. T., and Yamazaki, F., 2001. A proposal of instrumental seismic intensity scale compatible with MMI evaluated from three-component acceleration records, *Earthquake Spectra* **17**(4), 711–723.

Sokolov, V. Yu., 2002. Seismic intensity and Fourier acceleration spectra: revised relationship, *Earthquake Spectra* **18**, 161–187.

Sokolov, V. Yu., and Wald, D. J., 2002. Instrumental intensity distribution for the Hector Mine, California, and the Chi-Chi, Taiwan, earthquakes: a comparison of two methods, *Bull. Seismol. Soc. Am.* **92**, 2145–2162.

Wald, D. J., Quitoriano, V., Heaton, T. H., and Kanamori, H., 1999a. Relationships between peak ground acceleration, peak ground velocity and Modified Mercalli Intensity in California, *Earthquake Spectra* **15**, 557–564.

Wald, D. J., Quitoriano, V., Heaton, T. H., Kanamori, H., Serivner, V. W., and Worden, C. B., 1999b. TriNet "ShakeMaps": rapid generation of instrumental ground motion and intensity maps for earthquakes in southern California, *Earthquake Spectra* **15**, 537–555.

(Received 15 January 2007; accepted 15 October 2007)